A Modeling Framework to Quantify Impacts of Mobility Services on Multi-modal Transportation Systems: Methodology and a Case Study in Columbus, OH

Qiling Zou (https://orcid.org/0000-0003-2146-558X)
Sean Qian (https://orcid.org/0000-0001-8716-8989)

FINAL RESEARCH REPORT - August 28, 2023

Contract # 69A3551747111

Contents

1 Introduction

The rapid adoption of emerging technologies in vehicles, communications, and sensing is revolutionizing the way people travel. While people continue to choose the traditional transportation modes (e.g., driving and taking public transit) to complete their daily trips, more new transportation modes are becoming competing alternative traveling options due to their flexibility and convenience. For example, novel mobility services, including micro-transit, car sharing service, fix- or flex-route shared mobility services, have been proposed and experimented in some U.S. cities in order to improve the mobility in low-density residential areas (Grahn, Qian, & Hendrickson, 2021). The coexistence of such diversified transportation modes results in a very complex multi-modal transportation system. Although this complex system may enable innovative ways to combat traffic congestion and enhance travel reliability, it also presents a big challenge for transportation practitioners and researchers: how to effectively estimate and manage the vehicle and passenger flows in this multi-modal system in order to improve the overall network operational efficiency. One of the critical components that help address this challenge is accurately estimating the dynamic multi-modal origin-destination (O-D) demand, which plays a key role in transportation planning, operation, and management. To the authors' best knowledge, such studies are lacking in terms of understanding and estimating the dynamic OD demand for the multi-modal transportation network using sparse and partial flow observations. To fill this gap, this study presents a data-driven framework for multi-modal dynamic OD demand estimation (MMDODE) in large-scale networks. Based on the previous studies of one of the authors on the multi-modal dynamic user equilibrium (MMDUE) in (Pi, Ma, & Qian, 2019) and the multi-class dynamic OD demand estimation (MCDODE) in (Ma, Pi, & Qian, 2020), the MMDODE problem is formulated using a computational graph, and the forward-backward algorithm in (Ma et al., 2020) is further modified and extended to estimate the dynamic OD demand for the multi-modal transportation network efficiently and effectively.

The dynamic OD demand for the multi-modal transportation network represents the time-varying number of travelers departing from an origin and heading to a destination. Only with accurate fine-grained demand information as input can dynamic multi-modal transportation network models produce realistic path/link flows, revealing the spatio-temporal mobility patterns. Such results can help policymakers better understand the whole system from different perspectives such as departure/arrival patterns, mode choice of travelers, and public transit ridership. In addition, the dynamic OD demand is also beneficial for policymakers to evaluate the impacts of introducing new mode on the overall system and further devise appropriate operational strategies and pricing plans.

Given the importance of the dynamic OD demand, the dynamic OD estimation (DODE) has attracted substantial research attention over the past decades. Traditionally, it is formulated as a bi-level optimization problem with the goal of finding the optimal dynamic OD demand to minimize the discrepancy between the observations from the real world traffic data (e.g, vehicle counts) and the simulation results. The upper level aims to adjust the OD demand given the observed and the simulated path/link flows while the lower level relies on dynamic traffic assignment (DTA) models to output the simulation results with the OD demand as input. A large body of literature on the bi-level structure is available (Fisk, 1989; Yang, Sasaki, Iida, & Asakura, 1992; Florian & Chen, 1995; Jha et al., 2004). Researchers have also relaxed the bi-level problem to a single-level problem (C.-C. Lu, Zhou, & Zhang, 2013; Nie & Zhang, 2008).

Methods to solve the DODE problem can be generally classified into two categories: gradient-free and gradient-based approaches. The gradient-free methods are usually meta-heuristics such as genetic algorithms (Kim, Baek, & Lim, 2001; Kattan & Abdulhai, 2006; Vaze, Antoniou, Wen, & Ben-Akiva, 2009) and simulated annealing (Stathopoulos & Tsekeris, 2004). As for the gradient-based method, the Simultaneous Perturbation Stochastic Approximation (SPSA) method has been widely adopted, in which the finite differences are used to approximate the gradients of OD demand (Cipriani, Florian, Mahut, & Nigro, 2011; Ben-Akiva, Gao, Wei, & Wen, 2012; Cantelmo, Viti, Tampère, Cipriani, & Nigro, 2014; L. Lu, Xu, Antoniou, & Ben-Akiva, 2015). However, researchers also pointed out that the aforementioned meta-heuristics and the SPSA method belong to general-purpose optimization algorithms and have certain drawbacks in tackling the DODE problem. One of the main issues is that these general-purpose algorithms can be computational burdensome or even infeasible, especially in dealing with large-scale networks (Ma et al., 2020; Osorio, 2019). This is because they require multiple runs of expensive DTA models to generate sufficient information to drive the optimization. Research efforts have been devoted to the optimization algorithms with fewer DTA runs. For example, Lu et al. (C.-C. Lu et al., 2013) derive the gradient of the link flow with respect to path flow using cumulative curves. Osorio (Osorio, 2019) approximates the DTA model with a meta-model. In our past work, Ma et al. (Ma et al., 2020) proposes a novel computational-graph-based approach to linearly approximate the objective function with respect to the dynamic OD demand. Their method can not only deal with multiple vehicle classes and multi-source traffic data, but can also leverage multi-core CPUs or Graphics Processing Units (GPUs) to be efficiently applied to large-scale networks.

However, it can be found that most existing literature on the DODE has mainly focused on the transportation network with single travel mode (e.g., driving only), neglected the presence of other modes, and thus yielded the estimated OD demand

for single mode (e.g., dynamic OD vehicle demand for driving-only mode). Such single mode demand might not be sufficient to understand the whole transportation system since the real transportation can be multi-modal in nature. Meanwhile, there also lacks sufficient research on the general framework for the large-scale multi-modal transportation modeling, which can explicitly include both passenger flow and vehicular flow and holistically consider heterogeneous traffic flow and various travel modes (e.g., solo-driving, carpooling, ride-hailing, bus transit, railway transit, and park-and-ride) (Pi et al., 2019). Therefore, it remains a challenge to estimate the dynamic OD demand that matches multi-source spatio-temporal data and reflects the multi-modal traffic dynamics for a large-scale transportation network.

In light of this, this project aims to provide a general data-driven DODE framework for multi-modal transportation networks that incorporates the mode choice behavior of travelers and dynamic interactions among different modes in the network and facilitates further validation by emerging real-world data collected from the different components of the transportation system (e.g., roadway, public transit, and parking systems). Building on top of the MMDUE in (Pi et al., 2019) and the MCDODE in (Ma et al., 2020), this framework extends the computational graph approach to estimating the dynamic OD demand for multi-modal transportation networks with the advanced multi-modal DTA model capturing the underlying dynamics of both passenger flows and vehicular flows.

The main contributions of this study are summarized as follows:

1. It proposes a general formulation for estimating dynamic OD demand for multi-modal transportation networks. The formulation is represented on a computational graph such that the MMDODE can be solved for large-scale networks with multi-source traffic data. The MMDODE formulation can handle different forms of traffic data, such as passenger and vehicle flow, speed or trip cost.

2. It adopts a general simulation-based multi-modal DTA model to capture the flow dynamics of a multi-modal transportation network. This model considers travelers' mode choice and route choice behavior and explicitly models the propagation of mixed traffic flows including cars, trucks, buses, and passengers.

3. It presents a novel forward-backward algorithm to solve for the MMDODE formulation on the computational graph with simulation-based multi-modal DTA models. It transforms the MMDODE problem into a machine-learning task which can be solved effectively and efficiently with gradient descent algorithms.

4. It derives the gradient approximations of the objective function with respect to the dynamic OD demand considering the effects of the coexistence of multiple modes.

The remainder of this report is organized as follows. The modeling of multi-modal transportation network and the multi-modal dynamic user equilibrium condition are first introduced. It then presents the formulation and the solution algorithm for the MMDODE problem. A toy example is used to illustrate the effectiveness of the proposed framework. A case study is further carried out on a real-world regional multi-modal transportation network in Columbus, OH to analyze the impacts of mobility service on the whole network. Conclusions and future work are discussed at last.

2 Multi-modal dynamic traffic assignment

The DTA model is usually an essential part of the DODE problem. In the MM-DODE, a simulation-based multi-modal DTA model based on the MMDUE condition proposed by (Pi et al., 2019) is adopted as the underlying DTA model to generate path/flow patterns given the dynamic traveler OD demand as input.

2.1 Multi-modal transportation network

Although the MMDUE framework by (Pi et al., 2019) can accommodate many different modes, this paper focuses on three modes: driving (DR), taking bus transit (BT), and using mobility service with bus transit (MSBT). For the MSBT mode, travelers will take the mobility service to arrive at middle points of their trips first and then take the public transit to reach their final destinations. The middle points are usually set as the main transit hubs. To this end, a multi-modal transportation network is established, which consists of an auto network, a virtual bus network, and parking facilities (as shown in Figure 1).

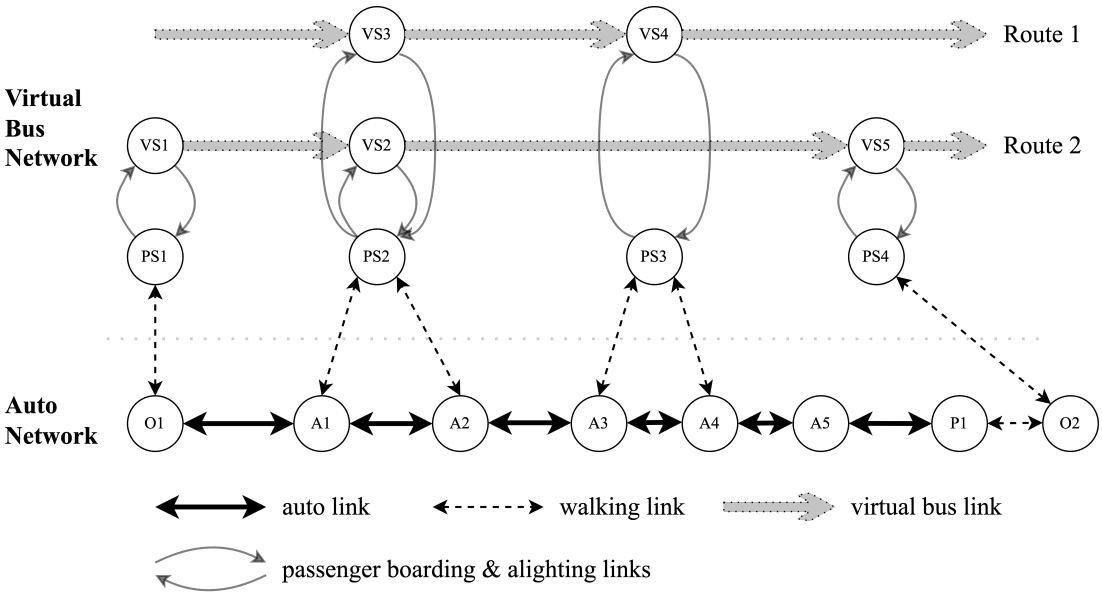

Figure 1: Illustration of a multi-modal transportation network: O: OD node; A: auto node; P: parking node; PS: physical bus stop; VS: virtual bus stop (Pi et al., 2019)

The auto network is the roadway network used by vehicles. The reason the bus network is called virtual is that buses share the same roadway network with other vehicles, so the virtual bus network is a combination of part of the auto network and bus stops. Two types of bus stops exist here: physical and virtual. A physical stop (PS) is a real bus stop where bus passengers board/alight the buses, and multiple routes

can traverse it. A virtual stop (VS), however, does not exist physically but is assumed here for the convenience of modeling and routing. A VS connects a PS to only one particular route and since a PS can be associated with multiple routes, a PS can be connected to multiple VSes. The links connecting a PS with a VS are called passenger boarding and alighting links. A virtual bus link is a link with endpoints being VSes and only corresponds to one particular route. A bus route is thus a sequence of one or more VSes (or virtual bus links). A bus follows a fixed route in this virtual bus network, but its travel cost/time is determined by the dynamic network loading (DNL) model with heterogeneous traffic flows, e.g., private cars, trucks, buses, and passengers. The parking facilities here refer to the near-destination parking lots/spaces. Travelers who choose the DR mode will drive all the way to their destination and have to park near their destinations and pay parking fees. In addition, the walking links are explicitly modeled to represent walking from origin to bus stops, from the middle destination to bus stops, transfer among bus stops, and from bus stops to the final destination.

With this representation, a path for a traveler for any OD pair can be composed of multiple components from different parts of this multi-modal network, depending on his/her mode choice. For example, a path for a traveler choosing the MSBT mode consists of auto links and nodes for the mobility service part, walking links for the transfer part, and bus links and stops for the bus riding part.

2.2 Generalized travel cost

To make modal choices, travelers need to make trade-offs among traffic congestion, convenience, parking fare, and expenditures to pay for travel. A logit model is adopted here to describe the mode choice behavior. For any O-D pair rs, the generalized travel cost function of DR, BT, and MSBT for a traveler departing at time t and taking the path k are defined in Eqs. 1, 2, and 3, respectively.

$$c^{rs}_{\mathrm{dr},k,t} = \alpha w^{rs}_{k,t} + \max[\gamma(t + w^{rs}_{k,t} - t^*), \beta(t^* - t - w^{rs}_{k,t})] + p_i/n + \Delta^{rs}_{k,t}(n) + \xi, \forall k \in P^{rs}_{\mathrm{dr}} \tag{1}$$

$$c^{rs}_{\mathrm{bt},k,t} = \alpha w^{rs}_{k,t} + \max[\gamma(t + w^{rs}_{k,t} - t^*), \beta(t^* - t - w^{rs}_{k,t})] + \delta^{rs} + \sigma^{rs}_{k,t}, \forall k \in P^{rs}_{\mathrm{bt}} \tag{2}$$

$$c^{rs}_{\mathrm{msbt},k,t} = \alpha w^{rs}_{k,t} + \max[\gamma(t + w^{rs}_{k,t} - t^*), \beta(t^* - t - w^{rs}_{k,t})] + \eta^{rs} + \omega^{rs}_{k,t}, \forall k \in P^{rs}_{\mathrm{msbt}} \tag{3}$$

where P_{dr}^{rs}, P_{bt}^{rs}, and P_{msbt}^{rs} denote the path sets for DR, BT, and MSBT from r to s, respectively; $w_{k,t}^{rs}$ denotes the actual travel time which might be the summation of driving time, possible transfer time, bus travel time, and all possible walking time during the trip; t^* is the target arrival time (e.g., standard work starting time); α is the unit cost of travel time; γ and β are the unit costs of time for arriving late and arriving early, respectively (this second term is also known as the schedule delay cost); p_i in Eq. 1 is the parking fee at parking area of the destination; n in Eq. 1 is the number of pooled travelers; $\Delta_{k,t}^{rs}(n)$ in Eq. 1 represents the carpooling impedance cost; ξ in Eq. 1 is an indicator of accessibility to a private car (if the traveler owns a car or has access to a private car then it can be set to 0, otherwise it should be a large constant); δ^{rs} in Eq. 2 represents the transit fare; $\sigma_{k,t}^{rs}$ in Eq. 2 is the possible perceived inconvenience cost of the transit mode associated with the crowding of transit route; η^{rs} and $\omega_{k,t}^{rs}$ in Eq. 3 are the fare and the possible perceived inconvenience cost of the MSBT mode, respectively. More terms can be incorporated to achieve a higher model fidelity (e.g., fuel costs and vehicle depreciation).

2.3 Multi-modal dynamic network loading

The actual travel time $w_{k,t}^{rs}$ in Eqs. 1-3 is obtained from the DNL process and can be further decomposed into summation of more detailed terms:

$$
\begin{aligned}
\text{DR}: w_{k,t}^{rs} &= w_{k,t}^{rs}(\text{car travel}) + w_{k,t'}^{rs}(\text{parking cruising}) + w_{k,t''}^{rs}(\text{walking}) \\
\text{BT}: w_{k,t}^{rs} &= w_{k,t}^{rs}(\text{walking}) + w_{k,t'}^{rs}(\text{transfer/waiting}) + w_{k,t''}^{rs}(\text{bus travel}) \\
&\quad + w_{k,t'''}^{rs}(\text{walking}) \\
\text{MSBT}: w_{k,t}^{rs} &= w_{k,t}^{rs}(\text{car travel}) + w_{k,t'}^{rs}(\text{transfer/waiting}) + w_{k,t''}^{rs}(\text{bus travel}) \\
&\quad + w_{k,t'''}^{rs}(\text{walking})
\end{aligned}
\tag{4}
$$

where $t < t' < t'' < t'''$ indicates the sequence of start time of a trip component along a path.

2.3.1 Car/bus travel time

Since the cars and the buses share the same auto network, the car/bus travel time in Eq. 4 is extracted from the DNL process considering the heterogeneous vehicular flow (i.e., light-duty vehicles like private cars and heavy-duty vehicles like buses and trucks). A multi-class traffic flow model proposed in (Z. S. Qian, Li, Li, Zhang, & Wang, 2017) is adopted here to capture the flow dynamics consisting of multiple classes of vehicles with distinct flow characteristics. Moreover, the multi-class cell transmission model (CTM) in (Z. S. Qian et al., 2017) is further modified to incorporate the passenger pick-up and drop-off behavior for buses.

Due to the size and the speed, buses are regarded as a special type of trucks in the DNL. Pi et al. (Pi et al., 2019) do not explicitly model buses but approximate buses with trucks in the traffic flow. This study extends their work by introducing the explicit bus modeling in the DNL. With the CTM link model, a bus stop (e.g., a PS and its associated VSes) is placed in one of the cells of the link depending on its geographic location. When a bus reaches the cell that contains a bus stop on its route, the bus will stop in this cell if either one or two of the following conditions are met: (1) there are in-vehicle passengers who will alight at this bus stop; (2) there are passengers at the bus stop who want to board and the number of in-vehicle passenger is less than the bus capacity. It is assumed that the bus stops in the bus bay of the bus stop, which separates the bus from the travel lanes of a roadway. In this way, the normal trucks behind the bus can pass the bus when the bus stops.

Since the DNL module is a mesoscopic one and all vehicles and passengers are realized using agent-based modeling techniques, this truck passing the bus in the simulation simply means that the position of the bus and that of the truck behind it are swapped. However, the vehicle travel time is computed using the cumulative curves from the DNL and it means that the first-in-first-out rule needs to hold (Nie & Zhang, 2008; Z. S. Qian et al., 2017; Pi et al., 2019). To this end, different cumulative curves are set up for normal vehicles (cars and trucks) and buses separately. For each link in auto link, there are one pair of arrival and departure curves for cars and the other pair for trucks. Although buses are treated as trucks in the DNL, the cumulative curves for the auto link do not account for buses. Instead, buses are counted using another pair of arrival and departure curves that are associated with the virtual bus link in the virtual bus network. So when the bus reaches or leaves a bus stop, the corresponding arrival and departure curves of the bus link will increase.

2.3.2 Travel time of other modes

Other travel time terms in Eq. 4 can be computed in a similar fashion with (Pi et al., 2019).

The parking cruising time depends on the expected parking occupancy in the destination area: $w^{rs}_{k,t}(\text{parking cruising}) = \varepsilon_i/(1 - e_i(t)/E_i)$, where the parking area i is on path k, and the ε_i is the average parking time of a parking area when it is empty, E_i is the total capacity of the parking area, and $e_i(t)$ is the time-dependent parking occupancy which can be either determined based on the DNL or estimated using historical parking data.

The transfer/waiting time $w^{rs}_{k,t'}(\text{transfer/waiting})$ can also be either determined based on the DNL or estimated using historical bus transit data.

The walking time is set to be proportional to the walking distance. $w^{rs}_{k,t}(\text{walking}) = l^{rs}_{k,t}/\bar{v}$, where $\bar{v}$ is the average walking speed and $l^{rs}_{k,t}$ is the total walking distance in the

route k at time t from r to s.

2.4 Multi-modal dynamic user equilibrium

In this study, given the traveler OD demand, the resultant path/flow pattern is assumed to reach the MMDUE condition, which read:

$$\begin{aligned} c^{rs}_{m,k,t} - \mu^{rs}_{m,t} &= 0 \quad \text{if } \forall k \in P^{rs}_m, f^{rs}_{m,k,t} > 0 \\ c^{rs}_{m,k,t} - \mu^{rs}_{m,t} &\geq 0 \quad \text{if } \forall k \in P^{rs}_m, f^{rs}_{m,k,t} = 0 \\ \frac{h^{rs}_{m,t}}{q^{rs}_t} &= \frac{\exp(-(\alpha^m + \beta_1 \mu^{rs}_{m,t}))}{\sum_{m'} \exp(-(\alpha^{m'} + \beta_1 \mu^{rs}_{m',t})} \\ &\forall r, s, t, m \end{aligned} \tag{5}$$

where $\mu^{rs}_{m,t}$ denotes the equilibrium cost of travel mode m from r to s departing at time t; $f^{rs}_{m,k,t}$ is the flow of path k in mode m from r to s departing at time t. $h^{rs}_{m,t} = \sum_{k \in P^{rs}_{m,t}} f^{rs}_{m,k,t}$ represents the flow of mode m from r to s departing at time t; $q^{rs}_t = \sum_{m \in \{\text{dr,bt,msbt}\}} h^{rs}_{m,t}$ represents the total flow from r to s departing at time t.

The MMDUE can further formulated as a variational inequality (VI) problem and can be solved using the closed-form gradient projection method proposed in (Pi et al., 2019), which is more efficient than the existing projection-based methods for large-scale networks.

To summarize, in the multi-modal dynamic traffic assignment model, with the dynamic traveler OD demand as input, the mode choice and route choice models yield the traveler path/flow based on initial network conditions. Then, the traveler path/flow is converted into vehicular and passenger flows based on their mode choices. The vehicular and passenger flows are further loaded onto the network, leading to updated network conditions (e.g., traffic states on links and at intersections, and waiting time at bus stops). The mode and route choices can be updated based on new network conditions, so do the passenger flow and vehicle flow. This procedure goes on until the equilibrium state is achieved. The whole process is shown in Figure 2.

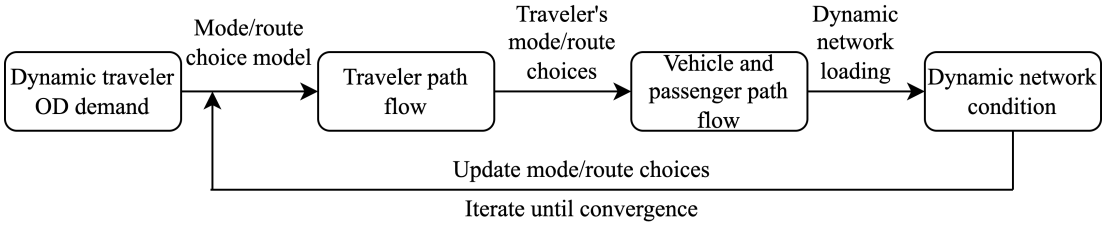

Figure 2: The whole process of the multi-modal dynamic traffic assignment

3 Multi-modal dynamic origin-destination estimation

With the multi-modal dynamic traffic assignment, this section discusses the MMDODE framework.

3.1 Formulation

The MMDODE aims to find the optimal dynamic traveler OD demand for the multi-modal transportation network to minimize the discrepancy between the observations from the real world traffic data and the simulation results. It is formulated as a bi-level optimization problem in Eqs. 6-23, which is an extension to the multi-class dynamic origin-destination estimation (MCDODE) in (Ma et al., 2020).

$$\begin{aligned}\min_{\{\mathbf{q},\mathbf{q}_{\text{truck}}\}} \mathscr{L} =& \mathscr{L}_1 + \mathscr{L}_2 + \mathscr{L}_3 + \mathscr{L}_4 \\ =& w_1(\|\mathbf{y}'_{\text{vehicle}} - \mathbf{y}_{\text{vehicle}}\|_2^2) \\ &+ w_2(\|\mathbf{y}'_{\text{passenger}} - \mathbf{y}_{\text{passenger}}\|_2^2) \\ &+ w_3(\|\mathbf{z}'_{\text{vehicle}} - \mathbf{z}_{\text{vehicle}}\|_2^2) \\ &+ w_4(\|\mathbf{z}'_{\text{bus}} - \mathbf{z}_{\text{bus}}\|_2^2)\end{aligned} \tag{6}$$

subject to

$$\begin{aligned}&\{\mathbf{w}^{\text{dr}}, \mathbf{w}^{\text{bt}}, \mathbf{w}^{\text{msbt}}, \mathbf{c}^{\text{dr}}, \mathbf{c}^{\text{bt}}, \mathbf{c}^{\text{msbt}}, \boldsymbol{\rho}^{\text{dr}}_{\text{car}}, \boldsymbol{\rho}^{\text{bt}}_{\text{passenger}}, \boldsymbol{\rho}^{\text{msbt}}_{\text{car}}, \boldsymbol{\rho}^{\text{msbt}}_{\text{passenger}}, \boldsymbol{\rho}_{\text{truck}}\} \\ &= \Lambda(\mathbf{f}^{\text{dr}}_{\text{car}}, \mathbf{f}^{\text{bt}}_{\text{passenger}}, \mathbf{f}^{\text{msbt}}_{\text{passenger}}, \mathbf{f}_{\text{truck}}, \mathbf{f}_{\text{bus}})\end{aligned} \tag{7}$$

$$\mathbf{q}^m = \mathbf{u}^m \mathbf{q} \quad \forall m \in \{\text{dr}, \text{bt}, \text{msbt}\} \tag{8}$$

$$\begin{aligned}&\mathbf{f}^m_i = \mathbf{p}^m_i \mathbf{q}^m \\ &\forall (m,i) \in \{(\text{dr}, \text{car}), (\text{bt}, \text{passenger}), (\text{msbt}, \text{passenger})\}\end{aligned} \tag{9}$$

$$\mathbf{f}_{\text{truck}} = \mathbf{p}_{\text{truck}} \mathbf{q}_{\text{truck}} \tag{10}$$

$$\begin{aligned}&\{\mathbf{u}^{\text{dr}}, \mathbf{u}^{\text{bt}}, \mathbf{u}^{\text{msbt}}, \mathbf{p}^{\text{dr}}_{\text{car}}, \mathbf{p}^{\text{bt}}_{\text{passenger}}, \mathbf{p}^{\text{msbt}}_{\text{passenger}}, \mathbf{p}_{\text{truck}}\} \\ &= \blacksquare(\mathbf{w}^{\text{dr}}, \mathbf{w}^{\text{bt}}, \mathbf{w}^{\text{msbt}}, \mathbf{c}^{\text{dr}}, \mathbf{c}^{\text{bt}}, \mathbf{c}^{\text{msbt}})\end{aligned} \tag{11}$$

$$\mathbf{x}^{\text{dr}}_{\text{car}} = \boldsymbol{\rho}^{\text{dr}}_{\text{car}} \mathbf{f}^{\text{dr}}_{\text{car}} \tag{12}$$

$$\mathbf{x}^{\text{bt}}_{\text{passenger}} = \boldsymbol{\rho}^{\text{bt}}_{\text{passenger}} \mathbf{f}^{\text{bt}}_{\text{passenger}} \tag{13}$$

$$\mathbf{x}_{\text{car}}^{\text{msbt}} = \boldsymbol{\rho}_{\text{car}}^{\text{msbt}} \mathbf{f}_{\text{passenger}}^{\text{msbt}} \tag{14}$$

$$\mathbf{x}_{\text{passenger}}^{\text{msbt}} = \boldsymbol{\rho}_{\text{passenger}}^{\text{msbt}} \mathbf{f}_{\text{passenger}}^{\text{msbt}} \tag{15}$$

$$\mathbf{x}_{\text{truck}} = \boldsymbol{\rho}_{\text{truck}} \mathbf{f}_{\text{truck}} \tag{16}$$

$$\mathbf{x}_{\text{car}} = \mathbf{x}_{\text{car}}^{\text{dr}} + \mathbf{x}_{\text{car}}^{\text{msbt}} \tag{17}$$

$$\mathbf{x}_{\text{passenger}} = \mathbf{x}_{\text{passenger}}^{\text{bt}} + \mathbf{x}_{\text{passenger}}^{\text{msbt}} \tag{18}$$

$$\mathbf{y}_{\text{vehicle}} = \sum_{i \in \{\text{car,truck}\}} \mathbf{L}_i \mathbf{x}_i \tag{19}$$

$$\mathbf{y}_{\text{passenger}} = \mathbf{L}_{\text{passenger}} \mathbf{x}_{\text{passenger}} \tag{20}$$

$$\mathbf{z}_{\text{vehicle}} = \sum_{i \in \{\text{car,truck}\}} \mathbf{M}_i \mathbf{t}_i \tag{21}$$

$$\mathbf{z}_{\text{bus}} = \mathbf{M}_{\text{bus}} \mathbf{t}_{\text{bus}} \tag{22}$$

$$\mathbf{q} \geq 0, \mathbf{q}_{\text{truck}} \geq 0 \tag{23}$$

For the sake of notation brevity and further tensor manipulation, all variables in the MMDODE are represented using tensors and are explained in Table 1. Other notations are listed in Table 2.

Eq. 6 is the objective function, which is to minimize the discrepancy between the observed traffic data and the estimated one. It consists of four parts: $\mathscr{L}_1$ and $\mathscr{L}_2$ are the losses related to traffic counts while $\mathscr{L}_3$ and $\mathscr{L}_4$ are the losses related to travel times. In addition to the vehicle-related data as in existing DODE literature, it also accounts for the bus transit data (i.e., passenger count and bus travel time). The parameters w_1, w_2, w_3, and w_4 are the weights to balance the scales of these four parts in the optimization.

Eq. 7 represents the multi-modal DNL process described in Section 2.3. The DNL function $\Lambda(\cdot)$ takes the multi-modal and multi-class path flow as input and out-

puts the spatio-temporal network conditions and the DAR matrices.

Eqs. 8 and 9 represent the mode choice and the route choice for travelers, respectively. Eq. 10 describes the route choice for trucks. It should be noted that the trucks serve as "background" traffic in the MMDODE and form mixed traffic flows with cars in the DNL in order to capture more realistic flow dynamics. The truck demand is also estimated along with the traveler demand. The mode choice and the route choice are obtained from a generalized function $\Psi(\cdot)$ in Eq. 11 which takes in the path travel time/cost defined in Eqs. 1-3 and outputs the mode choice matrix and the route choice matrix. The $\Psi(\cdot)$ can be either determined by exogenous mode/route choice data or chosen to be analytical models such as logit or probit models (Maher, Zhang, & Van Vliet, 2001).

Eqs. 12-16 represent the link traffic flow as the multiplication of the dynamic assignment ratio (DAR) matrix and the path flow. The element of the DAR matrix describes the link arrival/departure information with respect to total number of travelers using a certain path traveling between a certain OD pair departing at a certain time (Ma & Qian, 2018). The DAR matrix is obtained from the DNL results and varies with different travel demand input. Since obtaining the DAR matrix is often computationally challenging, the tree-based cumulative curves are adopted here to alleviate the computational burden to construct the DAR matrix (Ma et al., 2020).

Eqs. 17 and 18 describe the contributions of different modes to the link traffic flow. Specifically, Eq. 17 indicates that the car flow on the auto link comes from both the DR mode and the MSBT mode while Eq. 18 shows that both the BT mode and the MSBT mode contribute to the passenger flow on the bus link.

Eqs. 19 and 20 are the estimated flow for vehicles and passengers, respectively, while Eqs. 21 and 22 are the estimated travel time for vehicles and buses, respectively. It should be pointed out that $\mathbf{L}_i$ and $\mathbf{M}_i$ represent different aggregation of the link-level data. For example, the observed path travel time can be expressed as a summation of the travel time of multiple links. These variables expand the framework's flexibility to accommodate the observed data aggregated in various forms. More details and examples can be found in (Ma et al., 2020).

Eq. 23 is the non-negativity constraint for the demand.

Table 1: Tensors in MMDODE framework

Variable type	Vector	Dimension	Type	Description

OD demand	$\mathbf{q}, \mathbf{q}_{\text{truck}}$	$\mathbb{R}^{N\|K\|}$	Dense	Traveler OD demand and truck OD demand
Path flow	$\mathbf{f}_{\text{car}}^{\text{dr}}$	$\mathbb{R}^{N\Pi^{\text{dr}}}$	Dense	Path flow for car in DR mode
	$\mathbf{f}_{\text{passenger}}^{\text{bt}}$	$\mathbb{R}^{N\Pi^{\text{bt}}}$	Dense	Path flow for passenger in BT mode
	$\mathbf{f}_{\text{passenger}}^{\text{msbt}}$	$\mathbb{R}^{N\Pi^{\text{msbt}}}$	Dense	Path flow for passenger in MSBT mode
	$\mathbf{f}_{\text{truck}}$	$\mathbb{R}^{N\Pi_{\text{truck}}}$	Dense	Truck path flow
	$\mathbf{f}_{\text{bus}}$	$\mathbb{R}^{N\Pi_{\text{bus}}}$	Dense	Bus path flow
Link flow	$\mathbf{x}_{\text{car}}^{\text{dr}}$	$\mathbb{R}^{N\|A\|}$	Dense	Car link flow from DR mode
	$\mathbf{x}_{\text{car}}^{\text{msbt}}$	$\mathbb{R}^{N\|A\|}$	Dense	Car link flow from MSBT mode
	$\mathbf{x}_{\text{car}}$	$\mathbb{R}^{N\|A\|}$	Dense	Car link flow
	$\mathbf{x}_{\text{truck}}$	$\mathbb{R}^{N\|A\|}$	Dense	Truck link flow
	$\mathbf{x}_{\text{passenger}}^{\text{bt}}$	$\mathbb{R}^{N\|B\|}$	Dense	Passenger link flow from BT mode
	$\mathbf{x}_{\text{passenger}}^{\text{msbt}}$	$\mathbb{R}^{N\|B\|}$	Dense	Passenger link flow from MSBT mode
	$\mathbf{x}_{\text{passenger}}$	$\mathbb{R}^{N\|B\|}$	Dense	Passenger link flow
Link travel time	$\mathbf{t}_{\text{car}}, \mathbf{t}_{\text{truck}}$	$\mathbb{R}^{N\|A\|}$	Dense	Car and truck link travel time

	$\mathbf{t}_{\text{bus}}$	$\mathbb{R}^{N\lvert B\rvert}$	Dense	Bus link travel time
Path travel time and cost	$\mathbf{w}^{\text{dr}}, \mathbf{w}^{\text{bt}}, \mathbf{w}^{\text{msbt}}$	$\mathbb{R}^{N\Pi^m}$	Dense	Path travel time of three modes
	$\mathbf{c}^{\text{dr}}, \mathbf{c}^{\text{bt}}, \mathbf{c}^{\text{msbt}}$	$\mathbb{R}^{N\Pi^m}$	Dense	Path travel cost of three modes
Observed and estimated flow	$\mathbf{y}'_{\text{vehicle}}$, $\mathbf{y}_{\text{vehicle}}$	$\mathbb{R}^{\lvert C_a\rvert}$	Dense	Observed and estimated car and truck flow
	$\mathbf{y}'_{\text{passenger}}$, $\mathbf{y}_{\text{passenger}}$	$\mathbb{R}^{\lvert C_b\rvert}$	Dense	Observed and estimated passenger flow
Observed and estimated travel time	$\mathbf{z}'_{\text{vehicle}}$, $\mathbf{z}_{\text{vehicle}}$	$\mathbb{R}^{\lvert T_a\rvert}$	Dense	Observed and estimated car and truck travel time
	$\mathbf{z}'_{\text{bus}}$, $\mathbf{z}_{\text{bus}}$	$\mathbb{R}^{\lvert T_b\rvert}$	Dense	Observed and estimated bus link travel time
DAR matrix	$\boldsymbol{\rho}^{\text{dr}}_{\text{car}}$	$\mathbb{R}^{N\lvert A\rvert\times N\Pi^{\text{dr}}}$	Sparse	DAR matrix for cars in DR mode
	$\boldsymbol{\rho}^{\text{bt}}_{\text{passenger}}$	$\mathbb{R}^{N\lvert B\rvert\times N\Pi^{\text{bt}}}$	Sparse	DAR matrix for passengers in BT mode
	$\boldsymbol{\rho}^{\text{msbt}}_{\text{car}}$	$\mathbb{R}^{N\lvert A\rvert\times N\Pi^{\text{msbt}}}$	Sparse	DAR matrix for cars in MSBT mode
	$\boldsymbol{\rho}^{\text{msbt}}_{\text{passenger}}$	$\mathbb{R}^{N\lvert B\rvert\times N\Pi^{\text{msbt}}}$	Sparse	DAR matrix for passengers in MSBT mode
	$\boldsymbol{\rho}_{\text{truck}}$	$\mathbb{R}^{N\lvert A\rvert\times N\Pi_{\text{truck}}}$	Sparse	DAR matrix for trucks

Mode choice matrix	$\mathbf{u}^m$	$\mathbb{R}^{N\|K\|\times N\|K\|}$	Sparse	Mode choice matrix for each mode
Route choice matrix	$\mathbf{p}_{\text{car}}^{\text{dr}}$	$\mathbb{R}^{N\Pi^{\text{dr}}\times N\|K\|}$	Sparse	Route choice matrix for DR mode
	$\mathbf{p}_{\text{passenger}}^{\text{bt}}$	$\mathbb{R}^{N\Pi^{\text{bt}}\times N\|K\|}$	Sparse	Route choice matrix for BT mode
	$\mathbf{p}_{\text{passenger}}^{\text{msbt}}$	$\mathbb{R}^{N\Pi^{\text{msbt}}\times N\|K\|}$	Sparse	Route choice matrix for MSBT mode
	$\mathbf{p}_{\text{truck}}$	$\mathbb{R}^{N\Pi_{\text{truck}}\times N\|K\|}$	Sparse	Route choice matrix for trucks
Observation/link incidence matrix	$\mathbf{L}_{\text{car}},\ \mathbf{L}_{\text{truck}}$	$\mathbb{R}^{\|C_a\|\times N\|A\|}$	Sparse	Observation/link incidence matrix for cars and trucks
	$\mathbf{L}_{\text{passenger}}$	$\mathbb{R}^{\|C_b\|\times N\|B\|}$	Sparse	Observation/link incidence matrix for passengers
Link travel time portion matrix	$\mathbf{M}_{\text{car}}, \mathbf{M}_{\text{truck}}$	$\mathbb{R}^{\|T_a\|\times N\|A\|}$	Sparse	Link travel time portion matrices for cars and trucks
	$\mathbf{M}_{\text{passenger}}$	$\mathbb{R}^{\|T_b\|\times N\|B\|}$	Sparse	Link travel time portion matrix for passengers

3.2 Solution algorithm

In order to solve the MMDODE problem, the key is to obtain the gradients of the objective function with respect to the dynamic OD demands $\partial\mathscr{L}/\partial\mathbf{q}$ and $\partial\mathscr{L}/\partial\mathbf{q}_{\text{truck}}$

Table 2: Other notations in MMDODE framework

A	The set of all links of the auto network
B	The set of all links of the bus network
K	The set of all OD pairs
C_a, C_b	The set of indices of the observed flow for auto network and bus network
T_a, T_b	The set of indices of the observed travel time for auto network and bus network
Π^m	The number of all paths in mode m
Π_{truck}	The number of all paths for trucks
Π_{bus}	The number of all paths for buses
N	The total number of time intervals
i	The index of vehicle class and passenger
m	The index of mode

for the formulation above. The computational-graph-based approach proposed by (Ma et al., 2020) shows promising results in solving single-mode DODE problems on large-scale networks and is thus adopted here and further extended to the MMDODE problem.

First the MMDODE problem is cast into a computational graph representation, and Figure 3 describes the structure of the computational graph for MMDODE. A forward-backward algorithm running on the computational graph is used to obtain the gradients. The algorithm consists of two processes: the forward iteration and the backward iteration.

The forward iteration solves for the network conditions when the OD demand is given, while the backward iteration updates the OD demand when the network conditions are fixed. The forward-backward algorithm resembles some heuristic methods that solve the upper level and lower level problem iteratively but it also explores the analogy of a MMDODE problem and a machine learning task (i.e., training neural networks).

The forward iteration basically means solving the multi-modal DTA described in Section 2 and obtaining the mode/route choices (i.e., $\mathbf{u}^m$ in Eq. 8, $\mathbf{p}_i^m$ in Eq. 9, and $\mathbf{p}_{\text{truck}}$ in Eq. 10) and network conditions (i.e., , $\Lambda(\cdot)$ in Eq. 7).

The backward iteration is responsible for obtaining the gradients of the objective function via the backpropagation method. Taking the derivative of the objective function step by step and based on the chain rule, the gradients of interest are showed

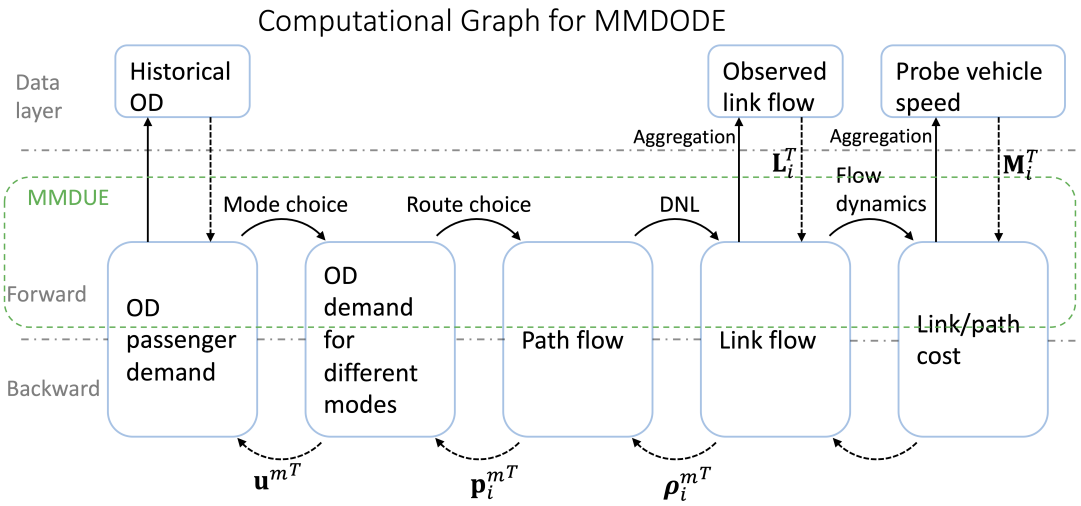

Figure 3: An illustration of the forward-backward algorithm

in Sections 3.2.1 and 3.2.2.

3.2.1 Gradients of flow-related losses

For the flow-related losses $\mathscr{L}_1$ and $\mathscr{L}_2$:

$$\frac{\partial \mathscr{L}_1}{\partial \mathbf{x}_{\text{car}}} = -2w_1 \mathbf{L}_{\text{car}}^T (\mathbf{y}'_{\text{vehicle}} - \sum_{i \in \{\text{car,truck}\}} \mathbf{L}_i \mathbf{x}_i) \tag{24}$$

$$\frac{\partial \mathscr{L}_1}{\partial \mathbf{x}_{\text{truck}}} = -2w_1 \mathbf{L}_{\text{truck}}^T (\mathbf{y}'_{\text{vehicle}} - \sum_{i \in \{\text{car,truck}\}} \mathbf{L}_i \mathbf{x}_i) \tag{25}$$

$$\frac{\partial \mathscr{L}_2}{\partial \mathbf{x}_{\text{passenger}}} = -2w_2 \mathbf{L}_{\text{passenger}}^T (\mathbf{y}'_{\text{passenger}} - \mathbf{L}_{\text{passenger}} \mathbf{x}_{\text{passenger}}) \tag{26}$$

$$\frac{\partial \mathscr{L}_1}{\partial \mathbf{x}_{\text{car}}^{\text{dr}}} = \frac{\partial \mathscr{L}_1}{\partial \mathbf{x}_{\text{car}}} \tag{27}$$

$$\frac{\partial \mathscr{L}_1}{\partial \mathbf{x}_{\text{car}}^{\text{msbt}}} = \frac{\partial \mathscr{L}_1}{\partial \mathbf{x}_{\text{car}}} \tag{28}$$

$$\frac{\partial \mathscr{L}_2}{\partial \mathbf{x}_{\text{passenger}}^{\text{bt}}} = \frac{\partial \mathscr{L}_2}{\partial \mathbf{x}_{\text{passenger}}} \tag{29}$$

$$\frac{\partial \mathscr{L}_2}{\partial \mathbf{x}_{\text{passenger}}^{\text{msbt}}} = \frac{\partial \mathscr{L}_2}{\partial \mathbf{x}_{\text{passenger}}} \tag{30}$$

$$\frac{\partial \mathscr{L}_1}{\partial \mathbf{f}_{\text{car}}^{\text{dr}}} = \boldsymbol{\rho}_{\text{car}}^{\text{dr}\ T} \frac{\partial \mathscr{L}_1}{\partial \mathbf{x}_{\text{car}}^{\text{dr}}} \tag{31}$$

$$\frac{\partial \mathscr{L}_2}{\partial \mathbf{f}_{\text{passenger}}^{\text{bt}}} = \boldsymbol{\rho}_{\text{passenger}}^{\text{bt}\ T} \frac{\partial \mathscr{L}_2}{\partial \mathbf{x}_{\text{passenger}}^{\text{bt}}} \tag{32}$$

$$\frac{\partial \mathscr{L}_1}{\partial \mathbf{f}_{\text{passenger}}^{\text{msbt}}} = \boldsymbol{\rho}_{\text{car}}^{\text{msbt}\,T} \frac{\partial \mathscr{L}_1}{\partial \mathbf{x}_{\text{car}}^{\text{msbt}}} \tag{33}$$

$$\frac{\partial \mathscr{L}_2}{\partial \mathbf{f}_{\text{passenger}}^{\text{msbt}}} = \boldsymbol{\rho}_{\text{passenger}}^{\text{msbt}\ \ T} \frac{\partial \mathscr{L}_2}{\partial \mathbf{x}_{\text{passenger}}^{\text{msbt}}} \tag{34}$$

$$\frac{\partial \mathscr{L}_1}{\partial \mathbf{f}_{\text{truck}}} = \boldsymbol{\rho}_{\text{truck}}{}^{T} \frac{\partial \mathscr{L}_1}{\partial \mathbf{x}_{\text{truck}}} \tag{35}$$

$$\frac{\partial \mathscr{L}_1}{\partial \mathbf{q}^{\text{dr}}} = \mathbf{p}_{\text{car}}^{\text{dr}\ \ T} \frac{\partial \mathscr{L}_1}{\partial \mathbf{f}_{\text{car}}^{\text{dr}}} \tag{36}$$

$$\frac{\partial \mathscr{L}_2}{\partial \mathbf{q}^{\text{bt}}} = \mathbf{p}_{\text{passenger}}^{\text{bt}\ \ T} \frac{\partial \mathscr{L}_2}{\partial \mathbf{f}_{\text{passenger}}^{\text{bt}}} \tag{37}$$

$$\frac{\partial \mathscr{L}_1}{\partial \mathbf{q}^{\text{msbt}}} = \mathbf{p}_{\text{passenger}}^{\text{msbt}\ \ T} \frac{\partial \mathscr{L}_1}{\partial \mathbf{f}_{\text{passenger}}^{\text{msbt}}} \tag{38}$$

$$\frac{\partial \mathscr{L}_2}{\partial \mathbf{q}^{\text{msbt}}} = \mathbf{p}_{\text{passenger}}^{\text{msbt}\ \ T} \frac{\partial \mathscr{L}_2}{\partial \mathbf{f}_{\text{passenger}}^{\text{msbt}}} \tag{39}$$

$$\frac{\partial \mathscr{L}_1}{\partial \mathbf{q}_{\text{truck}}} = \mathbf{p}_{\text{truck}}{}^{T} \frac{\partial \mathscr{L}_1}{\partial \mathbf{f}_{\text{truck}}} \tag{40}$$

$$\frac{\partial \mathscr{L}_1}{\partial \mathbf{q}} = \mathbf{u}^{\text{dr}T} \frac{\partial \mathscr{L}_1}{\partial \mathbf{q}^{\text{dr}}} + \mathbf{u}^{\text{msbt}T} \frac{\partial \mathscr{L}_1}{\partial \mathbf{q}^{\text{msbt}}} \tag{41}$$

$$\frac{\partial \mathscr{L}_2}{\partial \mathbf{q}} = \mathbf{u}^{\text{bt}T} \frac{\partial \mathscr{L}_2}{\partial \mathbf{q}^{\text{bt}}} + \mathbf{u}^{\text{msbt}T} \frac{\partial \mathscr{L}_2}{\partial \mathbf{q}^{\text{msbt}}} \tag{42}$$

It is noted that due to the presence of multiple modes, the gradients involve more terms and more intermediate steps compared to those for the single-mode DODE problem in (Ma et al., 2020). For example, Eq. 33 and Eq. 34 describe that the traveler flow in MSBT mode contributes to both vehicle and passenger link flows.

3.2.2 Gradients of travel-time-related losses

Similarly, for the travel-time-related losses $\mathscr{L}_3$ and $\mathscr{L}_4$:

$$\frac{\partial \mathscr{L}_3}{\partial \mathbf{t}_{\text{car}}} = -2w_3 \mathbf{M}_{\text{car}}^T (\mathbf{z}'_{\text{vehicle}} - \sum_{i \in \{\text{car,truck}\}} \mathbf{M}_i \mathbf{t}_i) \tag{43}$$

$$\frac{\partial \mathscr{L}_3}{\partial \mathbf{t}_{\text{truck}}} = -2w_3 \mathbf{M}_{\text{truck}}^T (\mathbf{z}'_{\text{vehicle}} - \sum_{i \in \{\text{car,truck}\}} \mathbf{M}_i \mathbf{t}_i) \tag{44}$$

$$\frac{\partial \mathscr{L}_4}{\partial \mathbf{t}_{\text{bus}}} = -2w_4 \mathbf{M}_{\text{bus}}^T (\mathbf{z}'_{\text{bus}} - \mathbf{M}_{\text{bus}} \mathbf{t}_{\text{bus}}) \tag{45}$$

$$\frac{\partial \mathscr{L}_3}{\partial \mathbf{x}_{\text{car}}} = \frac{\partial \bar{\Lambda}(\{\mathbf{x}_i\}_i)}{\partial \mathbf{x}_{\text{car}}} \frac{\partial \mathscr{L}_3}{\partial \mathbf{t}_{\text{car}}} \tag{46}$$

$$\frac{\partial \mathscr{L}_3}{\partial \mathbf{x}_{\text{truck}}} = \frac{\partial \bar{\Lambda}(\{\mathbf{x}_i\}_i)}{\partial \mathbf{x}_{\text{truck}}} \frac{\partial \mathscr{L}_3}{\partial \mathbf{t}_{\text{truck}}} \tag{47}$$

$$\frac{\partial \mathscr{L}_4}{\partial \mathbf{x}_{\text{truck}}} = \frac{\partial \bar{\Lambda}(\{\mathbf{x}_i\}_i)}{\partial \mathbf{x}_{\text{truck}}} \frac{\partial \mathbf{t}_{\text{bus}}}{\partial \mathbf{t}_{\text{truck}}} \frac{\partial \mathscr{L}_4}{\partial \mathbf{t}_{\text{bus}}} \tag{48}$$

$$\frac{\partial \mathscr{L}_4}{\partial \mathbf{x}_{\text{passenger}}} = \frac{\partial \mathbf{t}_{\text{bus}}}{\partial \mathbf{x}_{\text{passenger}}} \frac{\partial \mathscr{L}_4}{\partial \mathbf{t}_{\text{bus}}} \tag{49}$$

$$\frac{\partial \mathscr{L}_3}{\partial \mathbf{x}_{\text{car}}^{\text{dr}}} = \frac{\partial \mathscr{L}_3}{\partial \mathbf{x}_{\text{car}}} \tag{50}$$

$$\frac{\partial \mathscr{L}_3}{\partial \mathbf{x}_{\text{car}}^{\text{msbt}}} = \frac{\partial \mathscr{L}_3}{\partial \mathbf{x}_{\text{car}}} \tag{51}$$

$$\frac{\partial \mathscr{L}_4}{\partial \mathbf{x}_{\text{passenger}}^{\text{bt}}} = \frac{\partial \mathscr{L}_4}{\partial \mathbf{x}_{\text{passenger}}} \tag{52}$$

$$\frac{\partial \mathscr{L}_4}{\partial \mathbf{x}_{\text{passenger}}^{\text{msbt}}} = \frac{\partial \mathscr{L}_4}{\partial \mathbf{x}_{\text{passenger}}} \tag{53}$$

$$\frac{\partial \mathscr{L}_3}{\partial \mathbf{f}_{\text{car}}^{\text{dr}}} = \boldsymbol{\rho}_{\text{car}}^{\text{dr}\ T} \frac{\partial \mathscr{L}_3}{\partial \mathbf{x}_{\text{car}}^{\text{dr}}} \tag{54}$$

$$\frac{\partial \mathscr{L}_4}{\partial \mathbf{f}_{\text{passenger}}^{\text{bt}}} = \boldsymbol{\rho}_{\text{passenger}}^{\text{bt}\ T} \frac{\partial \mathscr{L}_4}{\partial \mathbf{x}_{\text{passenger}}^{\text{bt}}} \tag{55}$$

$$\frac{\partial \mathscr{L}_3}{\partial \mathbf{f}_{\text{passenger}}^{\text{msbt}}} = \boldsymbol{\rho}_{\text{car}}^{\text{msbt}\,T} \frac{\partial \mathscr{L}_3}{\partial \mathbf{x}_{\text{car}}^{\text{msbt}}} \tag{56}$$

$$\frac{\partial \mathscr{L}_4}{\partial \mathbf{f}_{\text{passenger}}^{\text{msbt}}} = \boldsymbol{\rho}_{\text{passenger}}^{\text{msbt}\ T} \frac{\partial \mathscr{L}_4}{\partial \mathbf{x}_{\text{passenger}}^{\text{msbt}}} \tag{57}$$

$$\frac{\partial \mathscr{L}_3}{\partial \mathbf{f}_{\text{truck}}} = \boldsymbol{\rho}_{\text{truck}}^{\ T} \frac{\partial \mathscr{L}_3}{\partial \mathbf{x}_{\text{truck}}} \tag{58}$$

$$\frac{\partial \mathscr{L}_4}{\partial \mathbf{f}_{\text{truck}}} = \boldsymbol{\rho}_{\text{truck}}^{\ T} \frac{\partial \mathscr{L}_4}{\partial \mathbf{x}_{\text{truck}}} \tag{59}$$

$$\frac{\partial \mathscr{L}_3}{\partial \mathbf{q}^{\text{dr}}} = \mathbf{p}_{\text{car}}^{\text{dr}\ T} \frac{\partial \mathscr{L}_3}{\partial \mathbf{f}_{\text{car}}^{\text{dr}}} \tag{60}$$

$$\frac{\partial \mathscr{L}_4}{\partial \mathbf{q}^{\text{bt}}} = \mathbf{p}_{\text{passenger}}^{\text{bt}\ T} \frac{\partial \mathscr{L}_4}{\partial \mathbf{f}_{\text{passenger}}^{\text{bt}}} \tag{61}$$

$$\frac{\partial \mathscr{L}_3}{\partial \mathbf{q}^{\text{msbt}}} = \mathbf{p}_{\text{passenger}}^{\text{msbt}\ T} \frac{\partial \mathscr{L}_3}{\partial \mathbf{f}_{\text{passenger}}^{\text{msbt}}} \tag{62}$$

$$\frac{\partial \mathscr{L}_4}{\partial \mathbf{q}^{\text{msbt}}} = \mathbf{p}_{\text{passenger}}^{\text{msbt}\ T} \frac{\partial \mathscr{L}_4}{\partial \mathbf{f}_{\text{passenger}}^{\text{msbt}}} \tag{63}$$

$$\frac{\partial \mathscr{L}_3}{\partial \mathbf{q}_{\text{truck}}} = \mathbf{p}_{\text{truck}}{}^T \frac{\partial \mathscr{L}_3}{\partial \mathbf{f}_{\text{truck}}} \tag{64}$$

$$\frac{\partial \mathscr{L}_4}{\partial \mathbf{q}_{\text{truck}}} = \mathbf{p}_{\text{truck}}{}^T \frac{\partial \mathscr{L}_4}{\partial \mathbf{f}_{\text{truck}}} \tag{65}$$

$$\frac{\partial \mathscr{L}_3}{\partial \mathbf{q}} = \mathbf{u}^{\text{dr}T} \frac{\partial \mathscr{L}_3}{\partial \mathbf{q}^{\text{dr}}} + \mathbf{u}^{\text{msbt}T} \frac{\partial \mathscr{L}_3}{\partial \mathbf{q}^{\text{msbt}}} \tag{66}$$

$$\frac{\partial \mathscr{L}_4}{\partial \mathbf{q}} = \mathbf{u}^{\text{bt}T} \frac{\partial \mathscr{L}_4}{\partial \mathbf{q}^{\text{bt}}} + \mathbf{u}^{\text{msbt}T} \frac{\partial \mathscr{L}_4}{\partial \mathbf{q}^{\text{msbt}}} \tag{67}$$

Special attention should be paid to Eqs. 46-49. The $\bar{\Lambda}(\cdot)$ is the dynamic link model, a part of the function $\Lambda(\cdot)$ in Eq. 7, and it takes the dynamic link flow as input and outputs the dynamic link travel time. It is assumed that the link travel time $\{\mathbf{t}_i\}_i$ is differentiable with respect to the incoming link flow. Most existing link models such as CTM, link queque model, and link transmission model are compatible.

However, no closed form exists for the derivative $\bar{\Lambda}(\{\mathbf{x}_i\}_i)/\mathbf{x}_i$. It is common practice to rely on approximation approaches (C.-C. Lu et al., 2013; Z. S. Qian, Shen, & Zhang, 2012; Ma et al., 2020). The approximation approach in (Ma et al., 2020) is adopted here. Specifically, $\bar{\Lambda}(\{\mathbf{x}_i\}_i)/\mathbf{x}_i$ is zero matrix when all links are not congested, and $\bar{\Lambda}(\{\mathbf{x}_i\}_i)/\mathbf{x}_i = \text{diag}(\tilde{\mathbf{x}}_i^{-1})$ when all links are congested. $\tilde{\mathbf{x}}_i^{-1}$ is the element-wise reciprocal of $\tilde{\mathbf{x}}_i$, which is the flow exiting from the head of each link for different vehicles. $\text{diag}(\tilde{\mathbf{x}}_i^{-1})$ is a square matrix with the diagonal elements being $\tilde{\mathbf{x}}_i^{-1}$ and other elements being zero. In the implementation, each entry of $\bar{\Lambda}(\{\mathbf{x}_i\}_i)/\mathbf{x}_i$ is chosen from either the zero matrix or $\text{diag}(\tilde{\mathbf{x}}_i^{-1})$ depending on whether the corresponding link is congested or not.

As for the bus link travel time in Eqs. 48 and 49, it assumes that each bus link travel time in $\mathbf{t}_{\text{bus}}$ consists of the bus travel time and the dwelling time at the bus stop:

$$t_{\text{bus},b} = \sum_{a \in \mathscr{S}(b)} r_a t_{\text{truck},a} + t_{\text{dwelling}} \tag{68}$$

where $\mathscr{S}(b)$ represents the set of auto links the bus link b covers and r_a represents the portion of the overlapped length between the bus link b and the auto link a to the whole length of the auto link a. This is because the bus stop can be in the middle of the auto link, and each bus link can overlap with multiple auto links. Since buses are treated as

trucks in the DNL, the actual time for bus traversing from one bus stop to the next one can be approximated by the corresponding truck travel time. The second term t_{dwelling} considers the dwelling time for a bus at a bus stop due to passenger pick-up or drop-off. The derivative of t_{dwelling} with respect to the passenger flow can be approximated as an additional boarding or alighting time incurred by an additional passenger.

Therefore, according to the chain rule, the gradients of the objective function with respect to the OD demand can be written as:

$$\frac{\partial \mathscr{L}}{\partial \mathbf{q}} = \frac{\partial \mathscr{L}_1}{\partial \mathbf{q}} + \frac{\partial \mathscr{L}_2}{\partial \mathbf{q}} + \frac{\partial \mathscr{L}_3}{\partial \mathbf{q}} + \frac{\partial \mathscr{L}_4}{\partial \mathbf{q}} \tag{69}$$

$$\frac{\partial \mathscr{L}}{\partial \mathbf{q}_{\text{truck}}} = \frac{\partial \mathscr{L}_1}{\partial \mathbf{q}_{\text{truck}}} + \frac{\partial \mathscr{L}_3}{\partial \mathbf{q}_{\text{truck}}} + \frac{\partial \mathscr{L}_4}{\partial \mathbf{q}_{\text{truck}}} \tag{70}$$

With the MMDODE formulation on a computational graph and the gradients above, the MMDODE problem can be solved as a machine learning/deep learning task with gradient descent methods. Ma et al. (Ma et al., 2020) only apply the stochastic gradient descent (SGD) and a handcrafted Adagrad in their work. The implementation of the optimization in this work is based on PyTorch (Paszke et al., 2019) and enables the direct use of more off-the-shelf algorithms such as RMSProp, Adam, NAdam, and Adamax. The code is opensourced on Github[1].

[1] https://github.com/maccmu/macposts

4 Toy network example

The proposed MMDODE framework is first illustrated using a small grid network. All the experiments are conducted on a desktop with Intel Core i7-7700 K CPU 4.20 GHz × 8, 32 GB RAM, and 500 GB SSD.

The small grid network is depicted in Figure 4 and has 4 OD pairs and 3 bus routes. The node 16 is set as the middle point for the MSBT mode, namely, travelers can first reach node 16 via mobility services and then switch to the bus transit to get to their final destinations. The auto links (1, 3), (14, 3), (15, 5), (2, 5), (9, 12), (9, 17), (11, 13), and (11, 18) are OD connectors and are modeled using the point queue model while the rest of links are modeled with the CTM and the identical triangular fundamental diagram (FD). In the FD, the length of the auto links (3, 4), (5, 4), (7, 6), (7, 8), (10, 9), and (10, 11) is 0.15 mile, the length of the auto links (4, 7) and (7, 10) is 0.25 mile, and the length of the auto links (3, 6), (5, 8), (6, 9), and (8, 11) is 0.55 mile. The free flow speed is 35 miles/hour for car and 25 miles/hour for truck. The flow capacity is 2,200 vehicles/hour for car and 1,200 vehicles/hour for truck, and the holding capacity is 200 vehicles/mile for car and 80 vehicles/mile for truck.

The analysis horizon is 150 minutes and divided into ten 15-minute time intervals (i.e., $N = 10$). To generate the ground truth data for training, the path flows for different modes $\mathbf{f}_{\text{car}}^{\text{dr}}$, $\mathbf{f}_{\text{passenger}}^{\text{bt}}$, $\mathbf{f}_{\text{passenger}}^{\text{msbt}}$, and $\mathbf{f}_{\text{truck}}$ are randomly sampled from uniform distributions Unif(0, 800), Unif(0, 50), Unif(0, 100), and Unif(0, 50), for each time interval, respectively. The mode choice and route choice portions are also randomly generated and treated as unknown, then we run the DNL to obtain the "true" network conditions.

The auto links (3, 4), (5, 4), (4, 7), (5, 8), (7, 6), and (7, 8) are chosen to generate the observed flow and travel time data for cars and trucks separately. All bus links are chosen to generate the observed passenger flow and bus travel time data. The observed data is then multiplied by $1+\varepsilon$ to get the observed data with noise, where $\varepsilon \sim \text{Unif}(-\xi, \xi)$ and $\xi \in [0, 1)$ represents the noise level. In this example, the noise level $\xi = 0.1$. The NAdam algorithm in PyTorch is used.

The change of loss $\mathscr{L}$ against the number of iterations is presented in Figure 5. To analyze the convergence of loss for cars, trucks, and passengers separately, the loss $\mathscr{L}$ is also decomposed into six components: car flow, truck flow, passenger flow, car travel time, truck travel time, and bus travel time, which are depicted in Figure 6. Note the losses are normalized to be within [0, 1]. The travel cost means the travel time. It can be seen that the total loss and the loss components all decrease as the iteration progresses.

The R-squared metric is also used to measure the goodness of fit between the true flow/cost and the estimated flow/cost. The scatter plots are shown in Figures 7

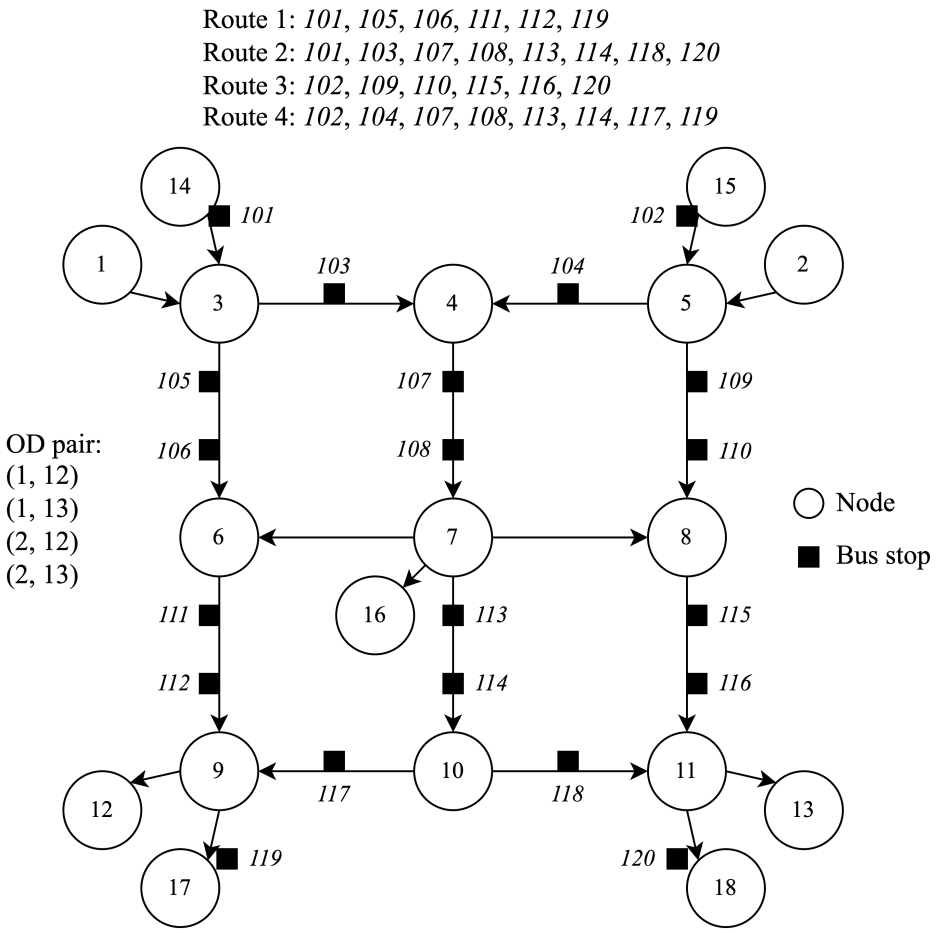

Figure 4: A small grid network

and 8. It can be seen that the R-squared of all flow and cost is above 0.9, except for the bus link travel time. The R-squared for the bus link travel time is about 0.8. The reasons are twofold: (1) the bus flow is relatively low compared to the other vehicle flow (only one bus every 15 mins for each route). This means that the other vehicles can largely affect the bus traveling in the DNL, making the task of estimating the bus travel time matching the true bus schedule challenging. (2) the bus link travel time is approximated by the truck travel time and the derivative of link travel time $\bar{\Lambda}(\{\mathbf{x}_i\}_i)/\mathbf{x}_i$ is also approximated by simulation rather than an accurate closed form. Due to the discretization and the randomness of the DNL process, such approximations can be noisy.

This small example shows that the proposed MMDODE framework yields accurate estimation of the dynamic OD demand for this small multi-modal network.

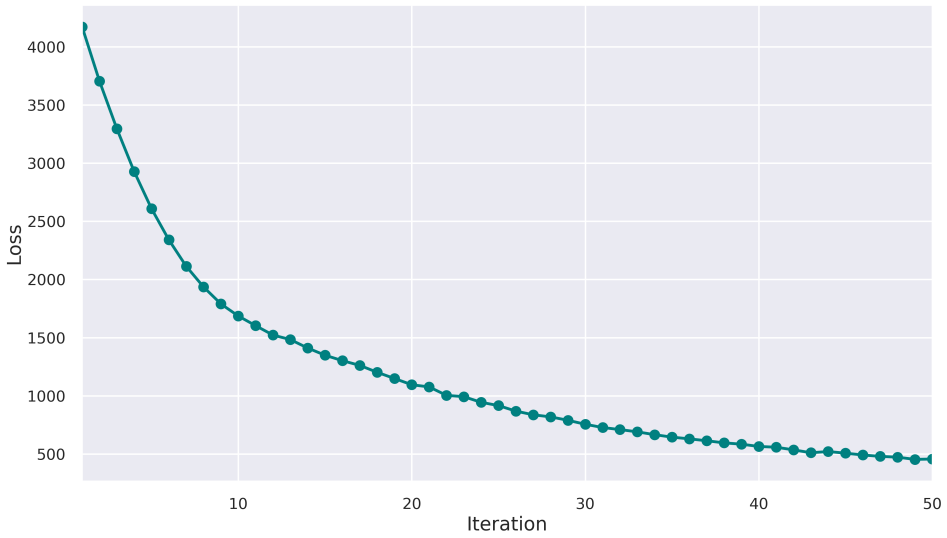

Figure 5: Convergence curve for the loss for the small grid network

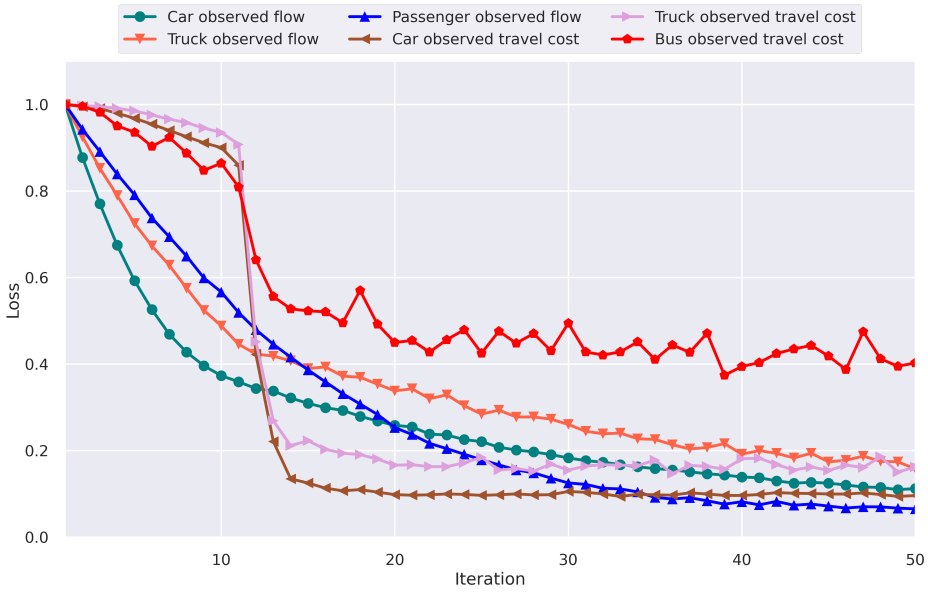

Figure 6: Decomposed convergence curve for the small grid network (normalized)

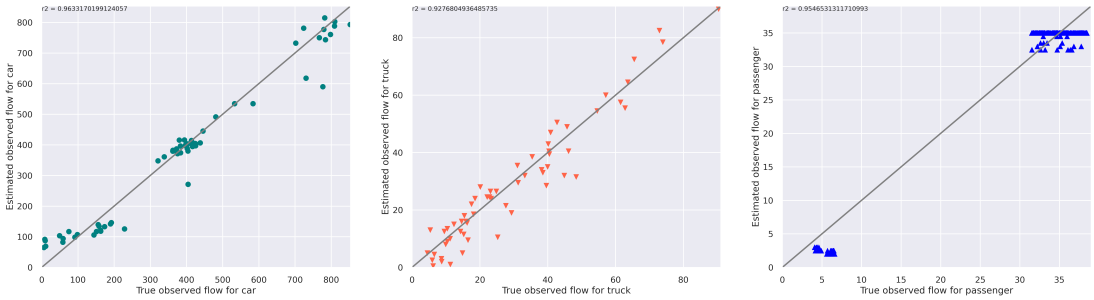

Figure 7: Estimated and "true" observed flow for cars, trucks, and passengers for the small grid network (unit: number of vehicles / 15 minutes or number of passengers / 15 minutes)

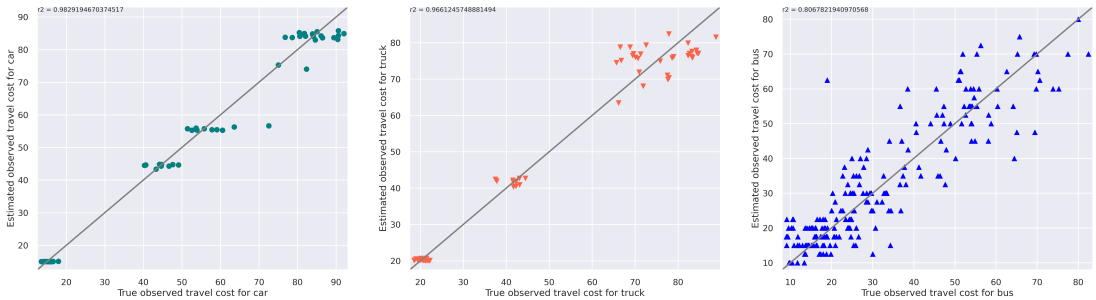

Figure 8: Estimated and "true" observed cost for cars, trucks, and passengers for the small grid network (unit: second)

5 Case study in Columbus, OH

5.1 OD demand estimation

The MMDODE framework is further applied to a large-scale network in central Ohio region (Figure 9), with Columbus located in the center, to test its feasibility and scalability. The parameters for this network are listed in the Table 3. For the MSBT mode, a total of 13 locations, where multiple bus routes cross, are selected as middle destinations. Due to data availability, only car, truck, and passenger flow data is used for the training. The traffic data is from multiple sources. The car and truck flow data is from Ohio Department of Transportation (ODOT), where car traffic volume counts are measured for all passenger cars and truck traffic volume counts includes all kinds of trucks at the measured location. There are a total of 883 auto links with valid car or truck count data. The bus passenger counts are from the Central Ohio Transit Authority (COTA). The average waiting time for each bus stop is set as 15 minutes. All the traffic flow observations are aggregated to a single data sample to represent the traffic state of a typical day. The NAdam algorithm is used to solve the MMDODE.

Table 3: Network parameters

Name	Value
Studying period	5:00 AM - 9:00 AM
Simulation unit interval	5 s
Length of time interval	15 min
Number of time intervals	16
Number of auto links	26,357
Number of nodes	8,706
Number of O-D pairs	11,092
Number of bus routes	60
Number of physical bus stops	2,493
Number of virtual bus stops	3,284
Number of bus links	3,224
Number of walking links	7,979

The MMDODE framework runs for 40 iterations. Each iteration takes about 30 minutes so the whole process takes around $30 \times 40 = 1200$ minutes. The convergence of the loss and the decomposed loss are shown in Figures 10 and 11, respectively. It can be observed that this proposed method converges fairly quickly for this large network.

Figure 9: MORPC network in central Ohio

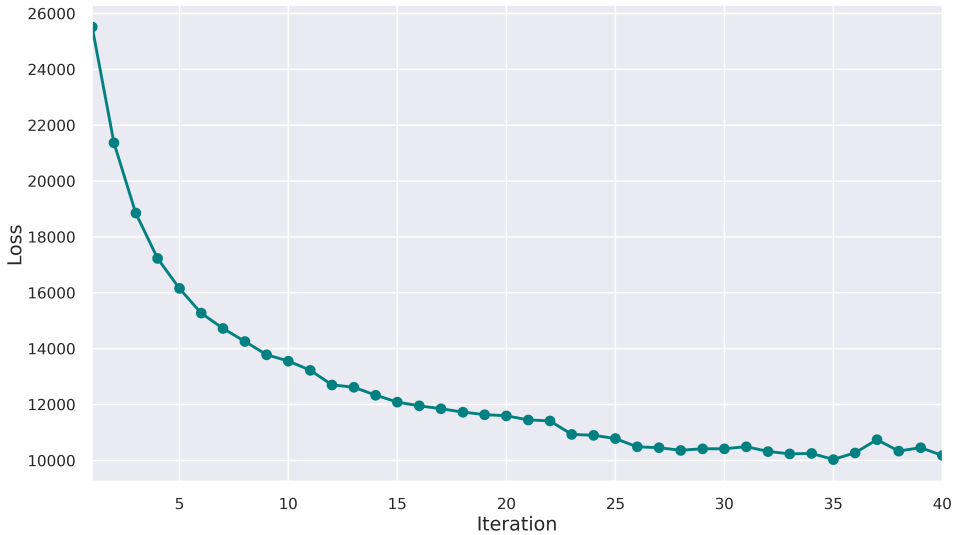

Figure 10: Convergence curve for the loss for 40 iterations for the network in the central Ohio region

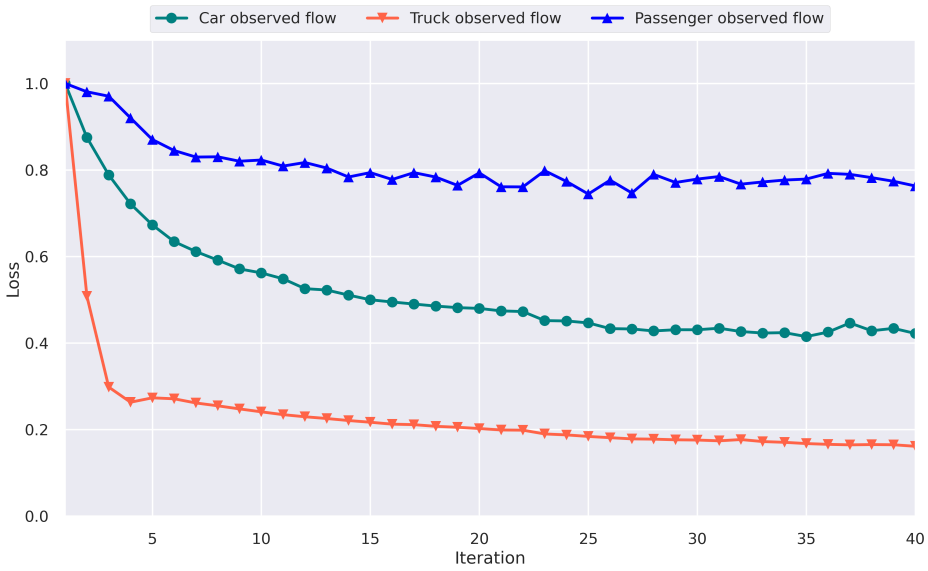

Figure 11: Decomposed convergence curve for the network in the central Ohio region (normalized)

The comparisons for the observed flow are presented in Figure 12. The R-squared is 0.81 and 0.84 for car and truck flow, respectively. But the R-squared for passenger flow is low, only 0.20. This is because the passenger flow is rather low compared to the vehicle flow. Again, due to the discretization and the randomness of the DNL, it is challenging to estimate the low traffic flow accurately. It can be observed that the loss for the passenger flow in Figure 11 does decrease but not as much as those for vehicle flows. This indicates that the proposed framework can minimize the passenger flow loss towards the right direction. One possible strategy to improve this result is using more comprehensive bus transit data. Note that only the passenger flow data is used in the training, but the passenger flow can be highly dependent on the bus schedule. It is an ongoing effort to integrate the bus schedule data to improve the passenger flow estimation (as in the small grid network above).

Overall, the results of the MMDODE framework is satisfactory for this large network in terms of the car and truck flow. Although the accuracy for the passenger flow estimation is not ideal, the loss function shows the correct decreasing trend, which means the proposed framework works to some extent but requires further improvement.

5.2 Impacts of mobility services

Based on the estimated OD demand, we run some scenario analyses to investigate the impacts of mobility services on the whole network. We assume travelers can

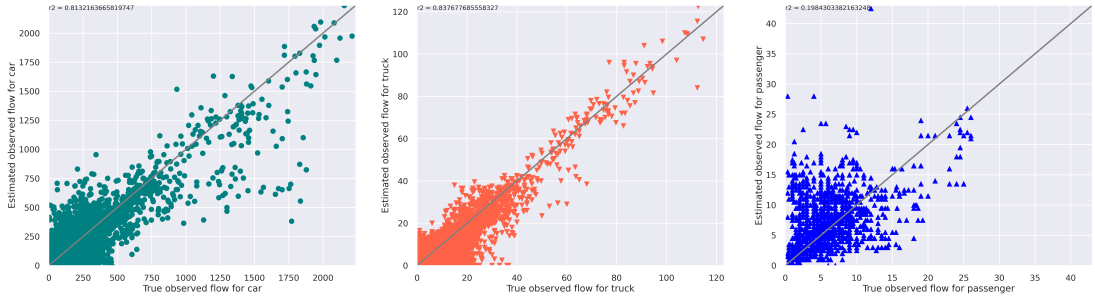

Figure 12: Estimated and true observed flow for cars, trucks, and passengers for the network in the central Ohio region (unit: number of vehicles / 15 minutes or number of passengers / 15 minutes)

make mode choices among driving, bus transit, and mobility services + bus transit. Due to the network size, we select 5,713 O-D pairs for demonstration because only these O-D pairs have more than two modes available. We select 13 locations, where multiple bus routes cross, as middle points for mobility services + bus transit. The study period is from 6 AM to 10 AM.

For travelers choosing the driving mode, we assume they will pay the parking fee ranging from $3 to $8 depending on the locations and their travel time includes the cruising time in the parking lot. The waiting time for mobility service and bus transit is set to 5 min and 10 min, separately. We also consider the effects of different demand levels.

The comparison of general metrics at the system level with and without mobility services is presented in Table 4, 5, and 6. We can find that introducing the mobility services can reduce emissions and improve the traffic efficiency. Note these results are based on a small amount of O-D demands, we expect that when the whole O-D pairs are considered, these reductions can be more significant.

Table 4: General metrics without mobility service

Demand multiplier	Fuel (gallon)	CO2 (ton)	HC (ton)	CO (ton)	NOX (ton)	VMT (mile)	VHT (hour)	Average Travel Time (min)
1	28,347.31	251.92	0.47	1.15	1.02	756,640.27	11,118.39	9.89
1.2	33,952.95	301.74	0.56	1.36	1.19	908,954.52	13,374.67	9.92

Table 5: General metrics with mobility service

Demand multiplier	Fuel (gallon)	CO2 (ton)	HC (ton)	CO (ton)	NOX (ton)	VMT (mile)	VHT (hour)	Average Travel Time (min)
1	27,204.17	241.76	0.45	1.10	0.98	725,547.32	10,665.20	9.53
1.2	30,230.59	268.66	0.50	1.22	1.08	807,665.05	11,881.53	9.59

Table 6: Reduction of general metrics when introducing mobility service

Demand multiplier	Fuel (gallon)	CO2 (ton)	HC (ton)	CO (ton)	NOX (ton)	VMT (mile)	VHT (hour)	Average Travel Time (min)
1	4.03%	4.03%	3.92%	3.74%	3.47%	4.11%	4.08%	3.64%
1.2	10.96%	10.96%	10.66%	10.33%	9.59%	11.14%	11.16%	3.31%

We also calculate the mode shares in different scenarios in Table 7. It shows that approximately 13% travelers choose mobility services + bus transit mode. This is also depicted in the flow pattern in Figure 13: more people use the bus transit when mobility service exists.

Table 7: Comparison of mode shares with and without mobility service

Demand multiplier		Driving	Bus transit	Mobility services + Bus transit
1	w/o mobility services	99.67%	0.33%	-
	w/ mobility services	86.84%	0.29%	12.87%
1.2	w/o mobility services	99.66%	0.34%	-
	w/ mobility services	86.93%	0.29%	12.78%

5.3 Mobility energy productivity metric

Mobility energy productivity (MEP) is a metric that quantifies the ability of an area's transportation system to connect individuals to goods, services, employment opportunities, and other activities while accounting for time, cost, and energy. It offers an innovative approach to characterize, measure, and inform the movement of people within a given location or region. The ability to quantify mobility using MEP has the potential to create more livable communities that offer transportation choices that are affordable and accessible, create economic opportunities, and lead to a higher quality of life for citizens.

$$o_{ikt} = \sum_j o_{ijkt} \frac{N^*}{N_j} \frac{f_j}{\sum_j f_j} \tag{71}$$

$$M_{ikt} = \alpha e_k + \beta t + \sigma c_k \tag{72}$$

$$MEP_i = \sum_k \sum_t (o_{ikt} - o_{ik(t-10)}) \exp(M_{ikt}) \tag{73}$$

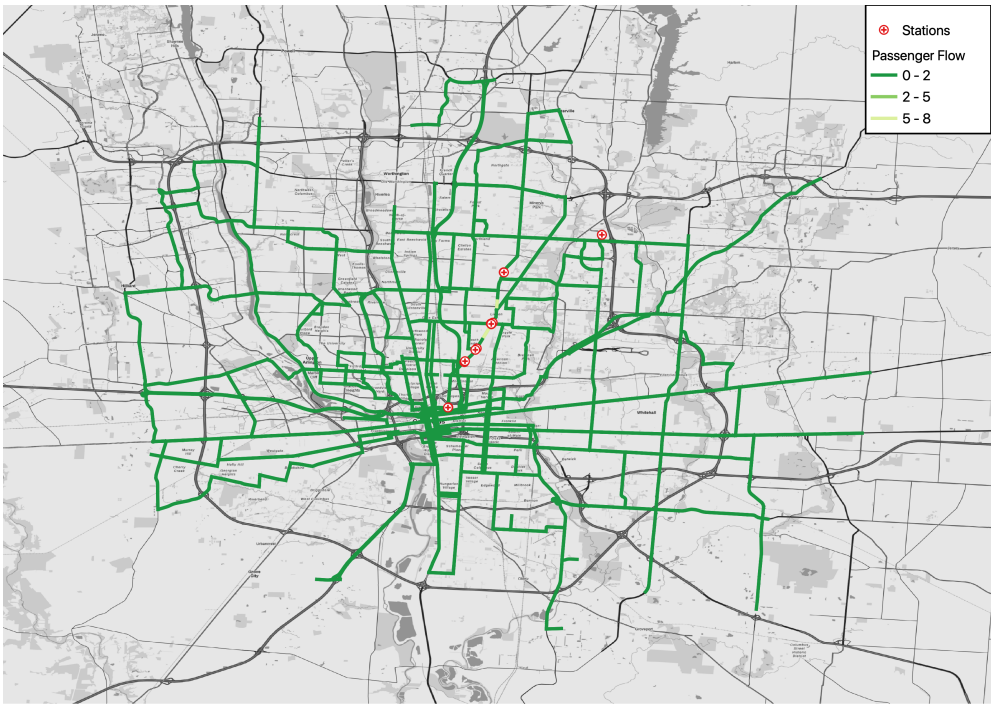

(a) Without mobility service

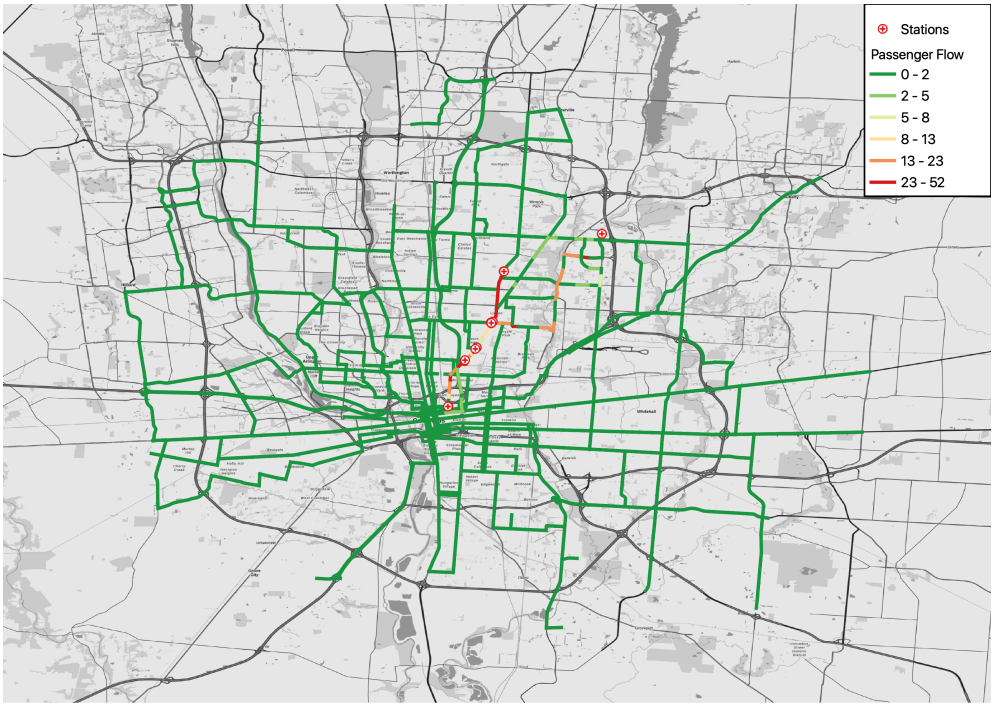

(b) With mobility service

Figure 13: Comparison of passenger flows with and without mobility service during 7:30AM - 7:45AM

Currently, we can calculate the MEP using the driving data, as shown in Figure 14. Integrating the bus transit data is an ongoing work.

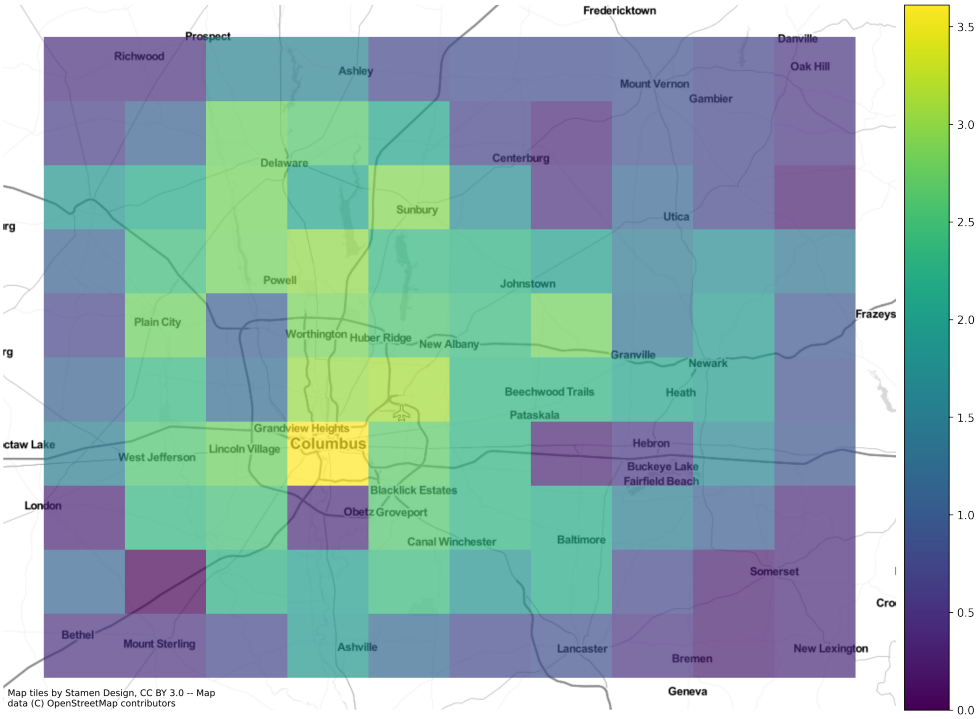

Figure 14: MEP for the central Ohio area based on driving data

6 Conclusion

Despite that the transportation is becoming more complex and multi-modal, the existing DODE frameworks usually focus on the single-mode transportation network. This project aims to develop a data-driven framework to estimate the dynamic OD demand for multi-modal transportation networks. By formulating the MMDODE problem on a computational graph, the problem can be solved by a forward-backward algorithm. In the forward iteration, the multi-modal dynamic traffic assignment problem is solved and the network conditions are obtained. In the backward iteration, the OD demand is updated by the backpropagation method with gradients extracted from the result of the forward iteration. The proposed framework provides a new perspective to view the MMDODE problem as a machine-learning task.

The effectiveness of this framework is tested on a small grid network as well as a real-world large-scale network. The experiment results indicate that this framework can yield satisfactory dynamic OD demand estimation results in terms of the car and truck flow. It also points out that accurately estimating the bus transit data can be challenging due to sparse bus and passenger flows and requires further research efforts. The preliminary results from the case study show that introducing mobility services has the potential to reduce emissions and improve the travel efficiency.

In future work, the estimation accuracy of the MMDODE framework can be enhanced in the following directions: (1) more bus transit data can be incorporated to improve the passenger flow estimation. Bus schedule can be embedded in the DNL to accurately simulate the bus arrival/departure; (2) the derivative of link travel time can be further improved by more accurate approximation methods, e.g., (Z. Qian & Zhang, 2011; Zhang & Qian, 2020).

Appendix

The code for MMDODE is made available at `https://github.com/maccmu/macposts`. The transportation network in Columbus, OH with estimated vehicle demand is available at `https://github.com/maccmu/macposts-examples`.

References

Ben-Akiva, M. E., Gao, S., Wei, Z., & Wen, Y. (2012). A dynamic traffic assignment model for highly congested urban networks. *Transportation research part C: emerging technologies*, *24*, 62–82.

Cantelmo, G., Viti, F., Tampère, C. M., Cipriani, E., & Nigro, M. (2014). Two-step approach for correction of seed matrix in dynamic demand estimation. *Transportation Research Record*, *2466*(1), 125–133.

Cipriani, E., Florian, M., Mahut, M., & Nigro, M. (2011). A gradient approximation approach for adjusting temporal origin–destination matrices. *Transportation Research Part C: Emerging Technologies*, *19*(2), 270–282.

Fisk, C. (1989). Trip matrix estimation from link traffic counts: The congested network case. *Transportation Research Part B: Methodological*, *23*(5), 331–336.

Florian, M., & Chen, Y. (1995). A coordinate descent method for the bi-level od matrix adjustment problem. *International Transactions in Operational Research*, *2*(2), 165–179.

Grahn, R., Qian, S., & Hendrickson, C. (2021). Improving the performance of first-and last-mile mobility services through transit coordination, real-time demand prediction, advanced reservations, and trip prioritization. *Transportation Research Part C: Emerging Technologies*, *133*, 103430.

Jha, M., Gopalan, G., Garms, A., Mahanti, B. P., Toledo, T., & Ben-Akiva, M. E. (2004). Development and calibration of a large-scale microscopic traffic simulation model. *Transportation Research Record*, *1876*(1), 121–131.

Kattan, L., & Abdulhai, B. (2006). Noniterative approach to dynamic traffic origin–destination estimation with parallel evolutionary algorithms. *Transportation research record*, *1964*(1), 201–210.

Kim, H., Baek, S., & Lim, Y. (2001). Origin-destination matrices estimated with a genetic algorithm from link traffic counts. *Transportation Research Record*, *1771*(1), 156–163.

Lu, C.-C., Zhou, X., & Zhang, K. (2013). Dynamic origin–destination demand flow estimation under congested traffic conditions. *Transportation Research Part C: Emerging Technologies*, *34*, 16–37.

Lu, L., Xu, Y., Antoniou, C., & Ben-Akiva, M. (2015). An enhanced spsa algorithm for the calibration of dynamic traffic assignment models. *Transportation Research Part C: Emerging Technologies*, *51*, 149–166.

Ma, W., Pi, X., & Qian, Z. (2020). Estimating multi-class dynamic origin-destination demand through a forward-backward algorithm on computational graphs. *Transportation Research Part C: Emerging Technologies*, *102747*.

Ma, W., & Qian, Z. S. (2018). Estimating multi-year 24/7 origin-destination demand using high-granular multi-source traffic data. *Transportation Research Part C: Emerging Technologies*, *96*, 96–121.

Maher, M. J., Zhang, X., & Van Vliet, D. (2001). A bi-level programming approach for trip matrix estimation and traffic control problems with stochastic user equilibrium link flows. *Transportation Research Part B: Methodological*, *35*(1), 23–40.

Nie, Y. M., & Zhang, H. M. (2008). A variational inequality formulation for inferring dynamic origin–destination travel demands. *Transportation Research Part B: Methodological*, *42*(7-8), 635–662.

Osorio, C. (2019). Dynamic origin-destination matrix calibration for large-scale network simulators. *Transportation Research Part C: Emerging Technologies*, *98*, 186–206.

Paszke, A., Gross, S., Massa, F., Lerer, A., Bradbury, J., Chanan, G., ... Chintala, S. (2019). Pytorch: An imperative style, high-performance deep learning library. In H. Wallach, H. Larochelle, A. Beygelzimer, F. d'Alché-Buc, E. Fox, & R. Garnett (Eds.), *Advances in neural information processing systems 32* (pp. 8024–8035). Curran Associates, Inc.

Pi, X., Ma, W., & Qian, Z. S. (2019). A general formulation for multi-modal dynamic traffic assignment considering multi-class vehicles, public transit and parking. *Transportation Research Part C: Emerging Technologies*, *104*(May), 369–389. doi: 10.1016/j.trc.2019.05.011

Qian, Z., & Zhang, H. M. (2011). Computing individual path marginal cost in networks with queue spillbacks. *Transportation Research Record*, *2263*(1), 9–18.

Qian, Z. S., Li, J., Li, X., Zhang, M., & Wang, H. (2017). Modeling heterogeneous traffic flow: A pragmatic approach. *Transportation Research Part B: Methodological*, *99*, 183–204.

Qian, Z. S., Shen, W., & Zhang, H. (2012). System-optimal dynamic traffic assignment with and without queue spillback: Its path-based formulation and solution via approximate path marginal cost. *Transportation research part B: methodological*, *46*(7), 874–893.

Stathopoulos, A., & Tsekeris, T. (2004). Hybrid meta-heuristic algorithm for the simultaneous optimization of the o–d trip matrix estimation. *Computer-Aided Civil and Infrastructure Engineering*, *19*(6), 421–435.

Vaze, V., Antoniou, C., Wen, Y., & Ben-Akiva, M. (2009). Calibration of dynamic traffic assignment models with point-to-point traffic surveillance. *Transportation Research Record*, *2090*(1), 1–9.

Yang, H., Sasaki, T., Iida, Y., & Asakura, Y. (1992). Estimation of origin-destination matrices from link traffic counts on congested networks. *Transportation Research Part B: Methodological*, *26*(6), 417–434.

Zhang, P., & Qian, S. (2020). Path-based system optimal dynamic traffic assignment: A subgradient approach. *Transportation Research Part B: Methodological*, *134*, 41–63.